



Cite this: *Energy Environ. Sci.*, 2024, 17, 2157

## Future environmental impacts of global hydrogen production†

Shijie Wei, \*<sup>a</sup> Romain Sacchi, <sup>b</sup> Arnold Tukker, <sup>ac</sup> Sangwon Suh<sup>d</sup> and Bernhard Steubing <sup>a</sup>

Low-carbon hydrogen ( $H_2$ ) will likely be essential in achieving climate-neutrality targets by 2050. This paper assesses the future life-cycle environmental impacts of global  $H_2$  production considering technical developments, regional feedstock supply, and electricity decarbonization. The analysis includes coal gasification, natural gas steam methane reforming, biomass gasification, and water electrolysis across 15 world regions until 2050. Three scenarios of the International Energy Agency are considered: (1) the Stated Policies Scenario (STEPS), (2) the Announced Pledges Scenario (APS) that entails aspirational goals in addition to stated policies, and (3) the Net Zero Emissions by 2050 Scenario (NZE). Results show the global average greenhouse gas (GHG) emissions per kg of  $H_2$  decrease from 14 kg CO<sub>2</sub>-eq. today to 9–14 kg CO<sub>2</sub>-eq. in 2030 and 2–12 kg CO<sub>2</sub>-eq. in 2050 (in NZE/STEPS). Fossil fuel-based technologies have a limited potential for emissions reduction without carbon capture and storage. At the same time, water electrolysis will become less carbon-intensive along with the low-carbon energy transition and can become nearly carbon-neutral by 2050. Although global  $H_2$  production volumes are expected to grow four to eight times by 2050, GHG emissions could already peak between 2025 and 2035. However, cumulative GHG emissions between 2020 and 2050 could reach 39 (APS) to 47 (NZE) Gt CO<sub>2</sub>-eq. The latter corresponds to almost 12% of the remaining carbon budget to meet the 1.5 °C target. This calls for a deeper and faster decarbonization of  $H_2$  production. This could be achieved by a more rapid increase in  $H_2$  produced via electrolysis and the additional expansion of renewable electricity. Investments in natural gas steam methane reforming with carbon capture and storage, as projected by the IEA, seem risky as this could become the major source of GHG emissions in the future, unless very high capture rates for CCS are assumed, and create a fossil fuel and carbon lock-in. Overall, to minimize climate and other environmental impacts of  $H_2$  production, a rapid and significant transition from fossil fuels to electrolysis and renewables accompanied by technological and material innovation is needed.

Received 11th November 2023,  
Accepted 29th January 2024

DOI: 10.1039/d3ee03875k

rsc.li/ees

### Broader context

Low-carbon hydrogen could help countries around the world to achieve their net-zero targets. Yet it is still unclear how the hydrogen economy will evolve and which environmental impacts it will cause. Prospective life cycle assessment can help identify solutions that can minimize environmental impacts of hydrogen production along transition scenarios. Guidance should consider existing and emerging technologies, possible temporal and regional differences, and broader socio-economic scenarios that determine the context of these developments. This paper considers both possible developments at the technology level as well as wider economic developments, such as the energy transition, based on shared socioeconomic pathways (SSPs) scenarios used (e.g., in the context of IPCC reports) to quantify the environmental impacts of global hydrogen production until 2050.

<sup>a</sup> Institute of Environmental Sciences (CML), Leiden University, 2333 CC Leiden, The Netherlands. E-mail: s.j.wei@cml.leidenuniv.nl

<sup>b</sup> Technology Assessment Group, Laboratory for Energy Systems Analysis, Paul Scherrer Institute, 5232 Villigen, Switzerland

<sup>c</sup> The Netherlands Organization for Applied Scientific Research TNO, The Netherlands

<sup>d</sup> Bren School of Environmental Science and Management, University of California, Santa Barbara, California 93106, USA

† Electronic supplementary information (ESI) available. See DOI: [10.1039/d3ee03875k](https://doi.org/10.1039/d3ee03875k)

### 1. Introduction

To limit global temperature increase at the end of this century to 1.5 degrees Celsius (°C) compared to pre-industrial times, it is necessary to achieve carbon neutrality in 2050 or earlier.<sup>1</sup> Hydrogen ( $H_2$ ) can be essential in transitioning to a net-zero energy system,<sup>2</sup> especially in the transport and heavy industry sectors.<sup>2,3</sup> As a result,  $H_2$  demand could increase six-fold by



2050.<sup>2</sup> Currently, H<sub>2</sub> is mainly produced as industrial feedstock from fossil fuels, primarily *via* coal gasification (CG) and steam reforming of natural gas (NG SMR).<sup>4</sup> Low-carbon alternatives that could cover the future demand for H<sub>2</sub> include water electrolysis using low-carbon electricity,<sup>5</sup> biomass gasification (BG), and fossil fuels coupled with carbon capture and storage (CCS). However, these technologies represent less than one percent of the global market today.<sup>2,4</sup> Further, low-carbon H<sub>2</sub> technologies may have environmental trade-offs that are not yet fully understood.<sup>6,7</sup>

Understanding the environmental impacts of emerging H<sub>2</sub> technologies is essential for adequately developing a roadmap and identifying an environmentally optimal trajectory to deploy H<sub>2</sub> technologies. A life-cycle perspective is required to obtain a complete picture of the environmental impacts of H<sub>2</sub> production. Life-cycle assessment (LCA) is suitable for assessing products and services' environmental performance throughout their life-cycle.<sup>8</sup>

Several LCA studies on H<sub>2</sub> production are available, *e.g.*, Bhandari *et al.*,<sup>9</sup> Siddiqui *et al.*,<sup>10</sup> Palmer *et al.*,<sup>11</sup> and Bauer *et al.*<sup>12</sup> These studies show that H<sub>2</sub> produced from water electrolysis powered by renewable electricity, biomass, and fossil fuel coupled with CCS leads to a substantial reduction in greenhouse gas (GHG) emissions compared with traditional production pathways but are also not free from environmental burdens. Considering that clean H<sub>2</sub> technology is an emerging solution within the energy landscape, several studies used prospective approaches in such LCAs. By incorporating expectations about process efficiency improvement, changes in properties of electrolyzers such as lifespan and material requirements, and possible decarbonization of the electricity mix, the prospective environmental impacts of H<sub>2</sub> production were assessed for various regions and countries. For example, Valente *et al.*<sup>13</sup> calculated the future carbon footprint of H<sub>2</sub> produced from NG SMR, BG, and water electrolysis by alkaline electrolyzers (AE) powered by grid and wind electricity in 2030 and 2050 in Spain. Delpierre *et al.*<sup>14</sup> compared the environmental impacts of wind power-based H<sub>2</sub> production by AE and proton exchange membrane electrolyzers (PEM) in the Netherlands in 2019 and 2050. Using a scenario generated by integrated assessment models (IAMs), coherently incorporating future dynamics of the energy-economy-land-climate system, Lamers *et al.*<sup>15</sup> quantified the environmental impacts of grid-coupled H<sub>2</sub> production by PEM and solid oxide electrolysis cell (SOEC) technology in the USA from 2020 to 2100.

Existing studies mainly focus on a limited number of H<sub>2</sub> production technologies in a single region, hindering a complete understanding of future environmental impacts across time and regions of different types of H<sub>2</sub> technologies, precisely when and where H<sub>2</sub> technology improvements and electricity decarbonization will likely occur. This paper aims to fill this knowledge gap by conducting an LCA of key H<sub>2</sub> production options and evaluating LCA results considering future H<sub>2</sub> technology improvements and developments in energy and other sectors. This assessment returns impacts per kg of H<sub>2</sub> for several environmental indicators across three development scenarios and 15 world regions. This can help guide H<sub>2</sub>

technology deployment and minimize its environmental impacts.

The main contributions of this paper are as follows:

(1) The life-cycle environmental impacts of H<sub>2</sub> production at the regional and global levels are quantified for the first time with a long-term perspective until 2050. This can provide valuable insights and decision support for H<sub>2</sub> technology developers and policymakers.

(2) We integrate the H<sub>2</sub> production scenarios into prospective LCA databases using the premise<sup>16</sup> framework and make this fully available online‡. This will allow future researchers to use our H<sub>2</sub> production scenarios directly for prospective LCA studies.

## 2. Methods and data

### 2.1. Goal and scope

Using attributional LCA, this paper aims to assess the environmental impacts caused by key H<sub>2</sub> production technologies from 2020 to 2050, using both one kg H<sub>2</sub> output and the future global H<sub>2</sub> demand as functional unit. Adopting a cradle-to-gate scope, a first functional unit is defined as one kg of gaseous H<sub>2</sub> output delivered at the user at a purity greater than 99.8% and 25–30 bar pressure. We further calculate impacts for a second functional unit, defined as total global production, according to scenarios further elaborated below.

As shown in Fig. 1, nine technologies are considered: CG, NG SMR, BG with or without CCS, and three variants of water electrolysis (*i.e.*, AE, PEM, and SOEC). We consider energy and material efficiency increases for future development and changes in these technologies' foreground life cycle inventory (LCI) data (see Section 2.2.1). Next, we model prospective changes in region-specific LCI background data with the IAM model REMIND (Regional Model of Investments and Development),<sup>17</sup> particularly for the energy system, using relevant shared socioeconomic pathway (SSP) scenarios. The future production volumes of these H<sub>2</sub> technologies until 2050 and associated technology shares are based on data from the International Energy Agency (IEA) in 3 scenarios: the Stated Policies Scenario (STEPS), the Announced Pledges Scenario (APS), and the Net Zero Emissions by 2050 Scenario (NZE) (see Section 2.2.2).<sup>2,4,18–20</sup> The detailed approach to the LCA is explained in the following sections.

### 2.2. Life cycle inventories of H<sub>2</sub> production

**2.2.1. Foreground data.** We discern nine technologies for H<sub>2</sub> production. We now discuss the unit process data for each technology and future changes therein. Data sources, key parameters, and assumed efficiency improvements over time are shown in Table 1. All unit process data can be found in the ESI† Section 1.

**CG with and without CCS.** In the CG route, the pulverized coal is partially oxidized with air or oxygen at high temperatures (800–1300 °C) and pressures of 30–70 bar, producing a syngas

‡ <https://github.com/premise-community-scenarios/hydrogen-prospective-scenarios>.



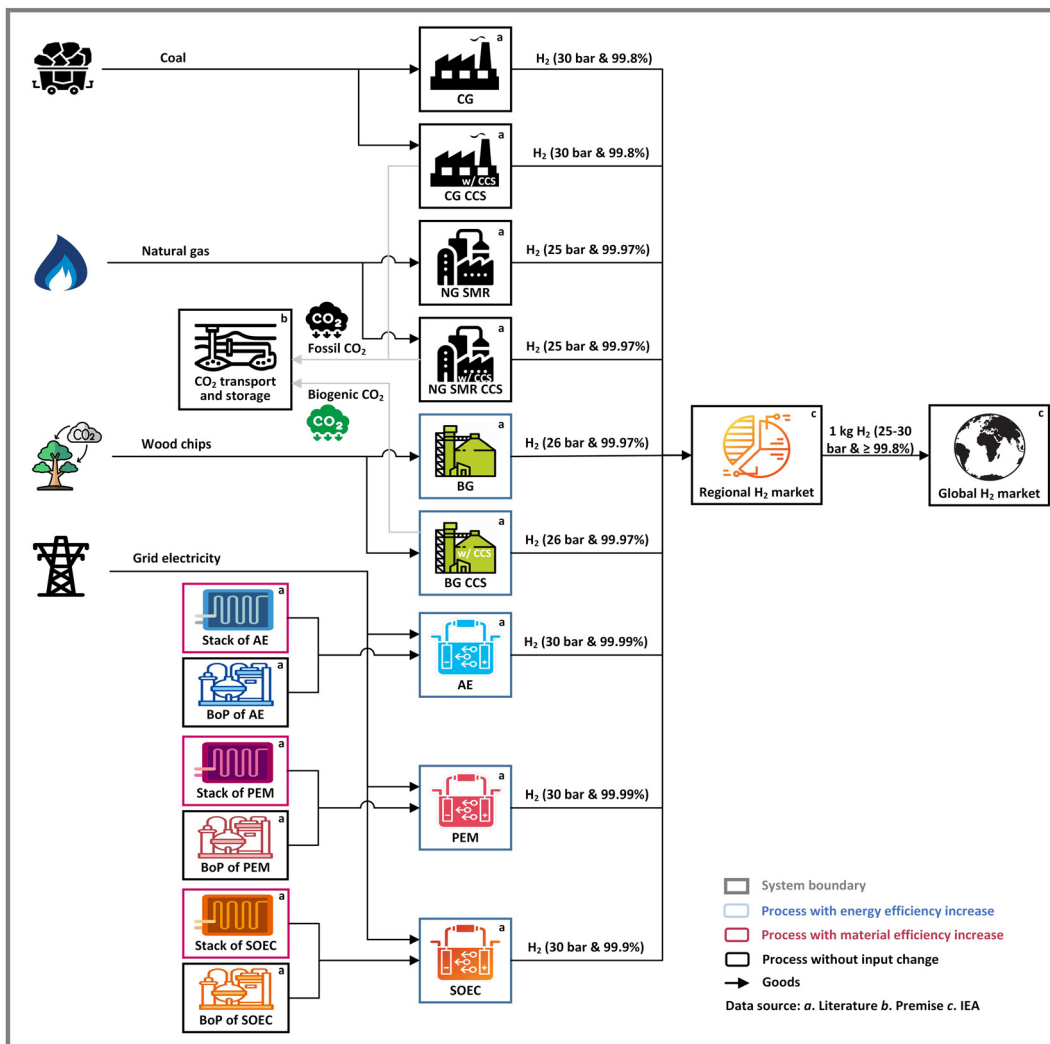
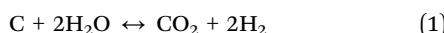


Fig. 1 The LCA model of H<sub>2</sub> production. <sup>§</sup> In this figure, *premise* is the model of PRospective EnvironMental Impact asSEment.<sup>16</sup> IEA = International Energy Agency database and reports.<sup>2,4,18–20</sup>

mixture composed of H<sub>2</sub>, carbon monoxide (CO), carbon dioxide (CO<sub>2</sub>) and small amounts of other gases and particles.<sup>30</sup> The raw syngas undergoes a water–gas shift reaction (WGSR) to enhance the H<sub>2</sub> yield. The overall reaction is shown in eqn (1).



After syngas scrubbing and H<sub>2</sub> separation using pressure swing adsorption (PSA), waste gases rich in CO<sub>2</sub> but also some H<sub>2</sub>, and CO can generate electricity to offset the plant's energy

<sup>§</sup> Processes of 'Coal', 'Wood chips', 'NG SMR', 'NG SMR CCS', 'BG', 'BG CCS', 'Stack of AE', 'Stack of PEM', 'Stack of SOEC', 'Regional H<sub>2</sub> market' and 'Global H<sub>2</sub> market' have been designed using images from Flaticon.com. The icon of CO<sub>2</sub> transport and storage is created by dDara from Noun Project. Processes of 'Grid electricity', 'Fossil CO<sub>2</sub>', 'Biogenic CO<sub>2</sub>', 'BoP of AE', 'BoP of PEM' and 'BoP of SOEC' are designed by Freepik. Processes of 'AE', 'PEM' and 'SOEC' are designed by Vecteezy.com. The image of 'Natural gas' is from <https://icon-library.com/icon/natural-gas-icon-0.html.html> > Natural Gas Icon # 235346. The image of 'CG' and 'CG CCS' is from <https://icon-library.com/icon/factory-icon-transparent-24.html.html> > Factory Icon Transparent # 96053.

use or be a co-product of the H<sub>2</sub> produced.<sup>31</sup> For large sources of CO<sub>2</sub> emissions like CG, NG SMR, and BG plants, CCS technology is expected to capture their CO<sub>2</sub> from waste gas by various capture technologies, including physical or chemical absorption processes. After compression, captured CO<sub>2</sub> is transported by pipeline, ship, rail, or truck and injected into deep geological formations such as saline aquifers or depleted oil and gas reservoirs.<sup>32</sup> It is assumed that the captured CO<sub>2</sub> can be sequestered underground safely for over 10 000 years so that it does not contribute to climate change.<sup>32,33</sup> The LCI data for CG and CG CCS, including hard coal, electricity, water, and CO<sub>2</sub> emissions, is from the National Renewable Energy Laboratory (NREL).<sup>21,24</sup> The LCI of infrastructure, waste treatment, and ammonia and hydrogen chloride emissions of CG were supplemented by data from Wokaun *et al.*<sup>22</sup> In the CG process, 3.18 kWh of electricity is produced as a co-product<sup>21</sup> and assumed to offset the environmental burdens of electricity from the grid using the substitution method.<sup>34,35</sup>

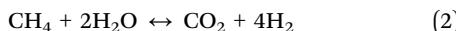
**Table 1** The overview of LCI source and efficiency improvement of H<sub>2</sub> production ways. Net efficiency refers to the ratios of the lower heating value of H<sub>2</sub> to that of feedstocks or electricity fed into the system

H <sub>2</sub> production technologies	Acronym of H <sub>2</sub> technologies	Lifespan of the H <sub>2</sub> plant (years)	Net efficiency (lower heating value) (%)			LCI and key parameters	
			2020	2030	2050	source	
Coal gasification w/o CCS	CG	30	54.5	54.5	54.5	21–23	
Coal gasification w/CCS	CG CCS	30	51.0	51.0	51.0	16 and 22–25	
Natural gas steam reforming w/o CCS	NG SMR	25	76.6	76.6	76.6	23 and 26	
Natural gas steam reforming w/CCS	NG SMR CCS	25	77.3 <sup>a</sup>	77.3	77.3	16, 23, 25 and 26	
Biomass gasification w/o CCS	BG	25	54.3	57.3	64.3	27 and 28	
Biomass gasification w/CCS	BG CCS	25	54.3	57.3	64.3	16, 25, 27 and 28	
Water electrolysis by alkaline electrolyzers	AE	20	67.0	68.0	75.0	23 and 29	
Water electrolysis by proton exchange membrane electrolyzers	PEM	20	58.0	66.0	71.0	23 and 29	
Water electrolysis by solid oxide electrolysis cell	SOEC	20	78.0 <sup>b</sup>	81.0	84.0	23 and 29	

<sup>a</sup> In NG SMR, the tail gas after H<sub>2</sub> separation must be burnt with air and additional natural gas in the reformer furnace. When CCS is adopted, the tail gas has less CO<sub>2</sub> and a higher heating value. The natural gas demand then decreases. As a result, NG SMR CCS has a higher net efficiency than NG SMR.<sup>26</sup> The overall energy efficiency of NG SMR CCS, considering the electricity consumption of CCS, is lower than that of NG SMR.<sup>b</sup> The electrical efficiency of water electrolysis is the system's efficiency with all utilities (electronics, pumps, safety equipment, infrastructure, etc.) and faradaic losses. For SOEC, electrical efficiency does not include the energy for steam generation.

Selexol solvent is used in the carbon capture technology for CG CCS,<sup>24</sup> and its LCI comes from Volkart *et al.*<sup>25</sup> It co-captures CO<sub>2</sub> and particulates, but other emissions remain unaffected.<sup>36</sup> With a capture rate of 90%, the captured CO<sub>2</sub> amounts to 20.39 kg per kg H<sub>2</sub>, leaving 2.27 kg CO<sub>2</sub> per kg H<sub>2</sub> uncaptured.<sup>24</sup> The electricity consumption for CO<sub>2</sub> capture, dehydration, and compression (to 150 bar) is 0.24 kW h per kg CO<sub>2</sub>.<sup>24,37,38</sup> The LCI of CO<sub>2</sub> transport and storage and their configurations are from Volkart *et al.*<sup>25</sup> and Sacchi *et al.*<sup>16</sup> CO<sub>2</sub> transport by pipeline was conservatively assumed to be over a distance of 400 km.<sup>25</sup> Saline aquifers are assumed as CO<sub>2</sub> storage sites as they have the largest storage potential.<sup>39</sup> A conservative assumption of CO<sub>2</sub> sequestration depth of 3 km is considered,<sup>40</sup> which is well beyond the 800 meters required to keep the CO<sub>2</sub> in a supercritical state.<sup>41</sup> The same CO<sub>2</sub> transportation and storage configuration is applied to the NG SMR CCS and BG CCS.

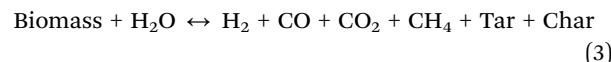
**NG SMR with and without CCS.** In NG SMR, methane reacts with steam using a catalyst at relatively high temperatures (650–1000 °C) and 5–40 bar pressures to produce CO and H<sub>2</sub>. Like coal gasification, the raw syngas undergoes a WGSR to recover more H<sub>2</sub> by reacting CO with steam.<sup>42</sup> In the WGSR, a high-temperature water-gas shift reactor is linked to an additional low-temperature one.<sup>26</sup> The overall reaction is represented by eqn (2). The excess steam is used for power generation to run the auxiliaries of the plant, and the surplus electricity goes to the grid.<sup>26</sup>



There are two sources of CO<sub>2</sub> in an SMR plant. One is the oxidation of the carbon in the feedstock during reforming and shift, accounting for 60–72% of the CO<sub>2</sub> emissions.<sup>26</sup> The other is tail gas combustion from PSA after H<sub>2</sub> separation, with air and additional natural gas in the reformer furnace. These CO<sub>2</sub> emissions can, in principle, be captured by a pre-combustion and a post-combustion CCS plant, respectively. But in NG SMR CCS, in practice, only a pre-combustion CCS plant is likely to be

used, being the most economical option.<sup>43</sup> The LCI of NG SMR and NG SMR CCS are from Antonini *et al.*<sup>26</sup> For NG SMR CCS, methyl diethanolamine (MDEA) is the solvent used to capture CO<sub>2</sub> with a capture rate of 90% (note that this excludes emissions from the reformer furnace).<sup>26</sup> The electricity consumption of CO<sub>2</sub> capture, dehydration, and compression is 0.18 kW h per kg CO<sub>2</sub>.<sup>26,37,38</sup>

**BG with and without CCS.** Like CG, BG consists of steam gasification, gas cleaning, WGSR, and H<sub>2</sub> separation *via* PSA.<sup>31</sup> It takes place at temperatures of 500–1400 °C and up to 33 bar pressures.<sup>44</sup> The BG uses an entrained flow gasifier as the gasification technology.<sup>27</sup> The overall reaction is represented by eqn (3). Except for mature technologies such as CG and NG SMR, other emerging H<sub>2</sub> production technologies are expected to improve efficiency. With the net efficiency increases, the wood chips input, corresponding CO<sub>2</sub> emissions, and required demand for CCS decrease. Except for the 5.5% of carbon losses during the pretreatment and gas cleanup,<sup>27</sup> the rest of the CO<sub>2</sub> emissions are assumed to be captured with a capture rate of 90% by the MDEA solvent. The LCI of the MDEA and water use for the CCS system are not given in Antonini *et al.*<sup>27</sup> and are sourced from Hospital-Benito *et al.*<sup>45</sup> The electricity requirement for CO<sub>2</sub> capture, dehydration, and compression is 0.19 kW h per kg CO<sub>2</sub>.<sup>27,37,38</sup> The biogenic CO<sub>2</sub> source coupled with CCS provides negative emissions.<sup>46</sup> For BG with and without CCS, wood chips are sourced from sustainably managed forests.<sup>27</sup>



**Water electrolysis.** Water electrolysis is a promising technology that utilizes low-carbon electricity to split water into H<sub>2</sub> and oxygen, as represented by eqn (4).<sup>47</sup> Water electrolysis can be subdivided into three electrolyzer technology types: AE, PEM, and SOEC. AE employing an aqueous potassium hydroxide solution is the most commercially mature technology and



operates at 60–90 °C.<sup>48</sup> PEM offers higher current densities, dynamic operation, and compact system design, but is also more expensive than AE and operates at lower temperatures of 50–100 °C.<sup>48,49</sup> Commercial rollout of PEM is expected in the next ten years at the megawatt-scale.<sup>50,51</sup> SOEC is an emerging technology that is still in the research and development stage.<sup>52,53</sup> It operates at high temperatures of 600–900 °C and could have the highest electrical efficiency among three main electrolyzers. If the required heat can be supplied from another exothermic process, *e.g.* ammonia production, this heat can be used instead of a dedicated heat supply to convert water into steam.<sup>29</sup>

All electrolyzers consists of stacks in series, where water electrolysis takes place, and a balance of plant (BoP). The BoP consists of all the supporting components and auxiliary systems, such as gas conditioning units, water and electricity feedstock conditioning units, and piping and instrumentation required to operate the electrolyzer.<sup>54,55</sup>



We use the initial LCI for water electrolysis, including the stack and BoP production of AE, PEM, and SOEC from Gerloff<sup>29</sup> and Bareiß *et al.*<sup>56</sup> Nafion, a sulfonated tetrafluoroethylene-based fluoropolymer-copolymer, is considered as membrane material for the PEM stack. It is assumed to be composed entirely of tetrafluoroethylene in Gerloff's research.<sup>29</sup> According to Simons *et al.*,<sup>57</sup> we further decompose 16 kg Nafion required for 1 MW PEM stack into 9.2 kg tetrafluoroethylene and 6.8 kg sulfuric acid. We further complete the LCI of the land footprint of electrolyzers, with 135 m<sup>2</sup> MW<sup>-1</sup>, 105 m<sup>2</sup> MW<sup>-1</sup>, and 55 m<sup>2</sup> MW<sup>-1</sup> for AE, PEM, and SOEC, respectively,<sup>58,59</sup> which is lacking in the initial LCI. In Gerloff,<sup>29</sup> feedstock water use per kg H<sub>2</sub> was set as 9 kg according to the stoichiometric coefficients. But in practice, more feedstock water should be used due to losses, up to 12 kg per kg H<sub>2</sub>.<sup>60</sup> This value is used in our inventory. The cooling water demands per kg H<sub>2</sub> are 0.088 m<sup>3</sup> for AE and PEM, and 0.645 m<sup>3</sup> for SOEC.<sup>29</sup> The electricity input in these three types of water electrolysis technologies is adjusted according to their respective efficiencies in 2020, as reported by IEA.<sup>23</sup> As the electrolyzers' efficiencies improve, electricity demand for producing a unit of H<sub>2</sub> reduces. In addition, the delivery purity and pressure of the H<sub>2</sub> from AE and SOEC are not apparent in Gerloff,<sup>29</sup> we further clarify this point in the ESI† Section 1.

While in the case of CG/NG SMR/BG, the environmental impacts are driven by fuel consumption and their direct emissions, the electrolyzer infrastructure is further considered due to its potentially significant impacts. To consider the plant infrastructure in the LCI, we first need to relate the cumulative production of H<sub>2</sub> over the plant's lifetime (assumed to be 20 years<sup>29</sup>) to the infrastructure requirements. The production amount of H<sub>2</sub> during a 20-year lifetime can be calculated as eqn (5):

$$P_i = \frac{C_i \times 1000 \times E_i \times L \times 8760 \times \text{CF}}{\text{LHV}_H} \quad (5)$$

where  $P_i$  denotes the H<sub>2</sub> production amount from water electrolysis technology  $i$  (kg);  $C_i$  is the capacity of the electrolyzer  $i$  (1 MW);  $E_i$  is

the efficiency of type  $i$  electrolyzer (%);  $L$  is the lifetime of the water electrolysis plant (20 years); 8760 is the number of hours in one year; CF is the capacity factor, indicating the total load hours in one year (0.95 due to the high availability of the grid electricity<sup>61</sup>); LHV<sub>H</sub> denotes the lower heating value of per kg H<sub>2</sub> (120 MJ kg<sup>-1</sup>, equal to 33.3 kW h kg<sup>-1</sup>).

As the functional unit is 1 kg H<sub>2</sub>, we calculate the electrolyzer (1 MW) input and divide it by the H<sub>2</sub> production amount over 20 years. The lifetime of the stack is generally shorter than that of BoP. Multiple stack replacements are required during the operation period of the electrolyzer system's whole lifespan.<sup>56</sup> In 2020, three stack replacements are required during the 20-year lifetime for AE and PEM, while SOEC needs nine times stack replacements.<sup>62</sup> As shown in Table 2, increasing research and development funding and induced production scale-up will lead to an extension of lifetime for stacks.<sup>63</sup> Note that the values used in this paper are slightly more conservative than those of the Hydrogen Analysis Production Models (H2A) developed by NREL.<sup>64</sup>

We also consider likely reductions of material use in the stack production itself due to manufacturing process improvements in the future. The changes in specific material requirements from 2020 to 2050 are shown in Table 3 (see also ESI† Table S20 for an example of how these values are included in the LCI data).

### 2.2.2. H<sub>2</sub> market developments until 2050

*Current H<sub>2</sub> production.* Although the global H<sub>2</sub> production volumes by technology and the H<sub>2</sub> production volumes in the 15 IEA regions were available for 2020,<sup>4,18</sup> there was no complete disaggregation of H<sub>2</sub> production by technology and region. For most regional H<sub>2</sub> markets in 2020, the production amounts for H<sub>2</sub> from unabated coal and natural gas are collected from the IEA reports,<sup>4,19</sup> while the production amounts of H<sub>2</sub> production from CCS projects and different types of water electrolysis are obtained from IEA's Hydrogen Production Projects Database.<sup>20</sup> However, data gaps for some regions had to be filled based on information from other sources. We refer to the detailed description of assumptions and data sources in Section 2.1 of the ESI†

*Future H<sub>2</sub> production.* For the future, we base our analysis on the STEPS, APS, and NZE scenarios for both the expected increase in H<sub>2</sub> production volumes and the technologies' market shares. The STEPS scenario considers existing and upcoming policies but does not foresee a drastic change in H<sub>2</sub> production.<sup>65</sup> This scenario corresponds to a global mean surface temperature (GMST) rise compared to pre-industrial levels of around 2.5 °C by 2100.<sup>18</sup> The APS and NZE scenarios foresee a significant rise in H<sub>2</sub> production. APS is a scenario that assumes that all climate commitments made by

Table 2 The stack lifetime of the different electrolyzer technologies

Lifespan (years)	2020	2030	2050	Source
AE	8.6	10.8	14.3	62
PEM	6.8	8.6	14.3	62
Values in the H2A	7 (2015)	10 (2040)		64
SOEC	2.3	5.7	10	62
Values in the H2A	4 (2015)	7 (2040)		64



Table 3 The material reduction in electrolyzer stack production

Materials (kg MW <sup>-1</sup> )	2020	2050	Ref.
AE, steel <sup>a</sup>	20194	8078	29 and 56
PEM, iridium	0.75	0.03	56
PEM, platinum	0.075	0.02	56
PEM, titanium	528	35	56
PEM, Nafion	16	2	56
PEM, activated carbon	9	4.5	56
PEM, steel	100	40	56
SOEC, steel	8976	3590	29 and 56

<sup>a</sup> According to Delpierre *et al.*,<sup>14</sup> steel consumption in the electrolyzer stack could decrease. The steel demand decrease in stack production of AE and SOEC is assumed to be the same as that of PEM: 60% from 2020 to 2050. Although the AE is a mature technology, there is a 4365–13 095 kg steel consumption range for a 1 MW stack by 2050.<sup>14,29</sup> Hence, this assumption seems reasonable.

governments worldwide, including Nationally Determined Contributions and longer-term net zero targets and targets for access to electricity and clean cooking, will be met in full and on time.<sup>65</sup> This scenario will keep the GMST in 2100 at around 1.7 °C.<sup>18</sup> The NZE scenario is a normative IEA scenario that shows a pathway for the global energy sector to achieve net zero CO<sub>2</sub> emissions by 2050. It assumes a higher pace of innovation in new and emerging technologies, a greater extent to which citizens are able or willing to change behavior, a higher availability of sustainable bioenergy, and a more effective international collaboration.<sup>65</sup>

Specifically, the global H<sub>2</sub> production volume increases from 70 Mt in 2020 to 121 Mt, 263 Mt, and 528 Mt in 2050 in the STEPS, APS, and NZE scenarios, respectively<sup>2,4,18</sup> (as shown in Fig. 4) to satisfy the demand for H<sub>2</sub> from traditional applications (industry and refining) and new uses (transport, buildings, agriculture, power generation, production of H<sub>2</sub>-derived fuels and H<sub>2</sub> blending in gas grid).<sup>2,66</sup> In the STEPS scenario, the increase stems mainly from conventional technologies, such as CG and NG SMR, as well as water electrolysis. There is a shift from conventional technologies to CCS and water electrolysis in the APS and NZE scenarios. Bioenergy-based H<sub>2</sub> does not play an important role. Its production volume is only 1.4 Mt in 2050 in the NZE scenario.<sup>2</sup> For this study, we estimate the future H<sub>2</sub> production mix in 15 IEA regions. We extrapolate the current production mix per region, as discussed above, with some adjustments based on IEA and literature data to meet the IEA global totals. These calculations and assumptions are provided in Section 2.2 of the ESI.† Although REMIND also models the production and use of H<sub>2</sub>, we do not use its projections for two reasons. First, its H<sub>2</sub> production volume in 2020 is minimal and not in line with actual production (*i.e.*, around 3 Mt). Second, REMIND limits the use of H<sub>2</sub> to the industry, building, and transport sectors,<sup>17</sup> which is not as comprehensive as the IEA scenarios.

**2.2.3. Background data.** Prospective LCI databases were used to represent future developments in other critical sectors and to avoid a temporal mismatch between foreground and background systems.<sup>67,68</sup> Corresponding to the IEA scenarios, three prospective LCI databases representing possible future

developments in 3 scenarios that combine SSPs and climate policies are used (see Table 4) based on their consistency in GMST rise by 2100: SSP2-NDC (~2.5 °C warming by 2100), SSP2-PkBudg1150 (1.6–1.8 °C warming by 2100) and SSP1-PkBudg500 (~1.3 °C warming by 2100). The IAM community developed SSPs to describe how global society, demographics, economics, and technology might change over this century.<sup>69</sup> In the narrative of the *middle-of-the-road* scenario (SSP2),<sup>69</sup> socioeconomic factors follow their historical trends with no notable shifts.<sup>70</sup> The SSP1 narrative depicts a world that aims for green growth (sustainable development).<sup>69</sup> The high energy efficiency and shares of renewable energy make the 1.5 °C target more credible.<sup>71</sup> The 'NDC' scenario refers to implementing all emission reductions and other mitigation commitments of the Nationally Determined Contributions under the Paris Agreement. 'PkBudg1150' and 'PkBudg500' are more stringent climate policy scenarios that limit cumulative emissions to 1150 Gt and 500 Gt CO<sub>2</sub> equivalents for the period 2020–2100, which is consistent with the GMST rise of 2 °C and 1.5 °C by 2100.<sup>17</sup>

The LCI background databases are derived from a combination of the ecoinvent v3.8 (system model "Allocation, cut-off by classification") database<sup>72</sup> and the REMIND model<sup>17</sup> (among the five IAM used for deriving marker scenarios of SSPs<sup>69</sup>) by using the open-source Python library premise v1.5.8.<sup>16</sup> In these databases, the electricity sector by region is updated. Updating the electricity inventories implies an alignment of regional electricity production mixes and efficiencies for several electricity production technologies, including CCS technologies and photovoltaic panels.<sup>15,16</sup> To match the market data provided by the IEA to the regional disaggregation of the REMIND-based prospective LCI background data from premise, a regional correspondence is established (the matching of regions and a list of countries associated with these regions can be found in Section 3 in the ESI†). Process inputs from the same region as the H<sub>2</sub> production region are paired based on this correspondence, if available, the rest of the world or the global level is used otherwise.

### 2.3. Life cycle impact assessment

Characterization factors provided by the IPCC's Fifth Assessment Report are used to quantify global warming potentials with a time horizon of 100 years.<sup>73</sup> To those we add characterization factors for the uptake and release of biogenic CO<sub>2</sub> (*i.e.*, -1 and +1, respectively) and H<sub>2</sub> emissions (*i.e.*, +11), needed to correctly consider negative emissions technologies, such as bioenergy with CCS, and H<sub>2</sub> leakages, as H<sub>2</sub> can act as an

Table 4 The matching of scenarios between IEA and REMIND. GMST is the global mean surface temperature

IEA <sup>18,65</sup>		REMIND <sup>17</sup>			
Sector	Scenario	GMST increase by 2100 (°C)	Sector	Scenario	
H <sub>2</sub>	STEPS	~2.5	Global	SSP2-NDC	~2.5
	APS	~1.7	Economy	SSP2-PkBudg1150	1.6–1.8
	NZE	~1.4		SSP1-PkBudg500	~1.3



indirect greenhouse gas.<sup>74</sup> 15 other environmental indicators are quantified by the method of EF v3.0:<sup>75</sup> acidification (mol H<sup>+</sup>-eq.), ecotoxicity: freshwater (CTUe), resource use: energy carriers (MJ), eutrophication: aquatic freshwater (kg P-eq.), eutrophication: aquatic marine (kg N-eq.), eutrophication: terrestrial (mol N-eq.), human toxicity: cancer effects (CTUh), human toxicity: non-cancer effects (CTUh), ionizing radiation: human health (kBq U<sup>235</sup>), land use (dimensionless), resource use: minerals and metals (kg Sb-eq.), ozone depletion (kg CFC-11-eq.), particulate matter (disease incidences), photochemical ozone formation (kg NMVOC-eq.) and water use (kg world eq.

deprived). Life cycle impact assessment results are calculated with the Activity Browser.<sup>76</sup> The superstructure approach<sup>77</sup> is used to handle LCA calculations with multiple foreground scenarios and prospective LCI background databases (representing the different REMIND scenarios across time).

### 3. Results and discussion

#### 3.1. Prospective GHG emissions of H<sub>2</sub> production pathways

Fig. 2 shows the GHG emissions of various H<sub>2</sub> technologies per kg H<sub>2</sub> produced in China, the USA, and the EU from 2020 to

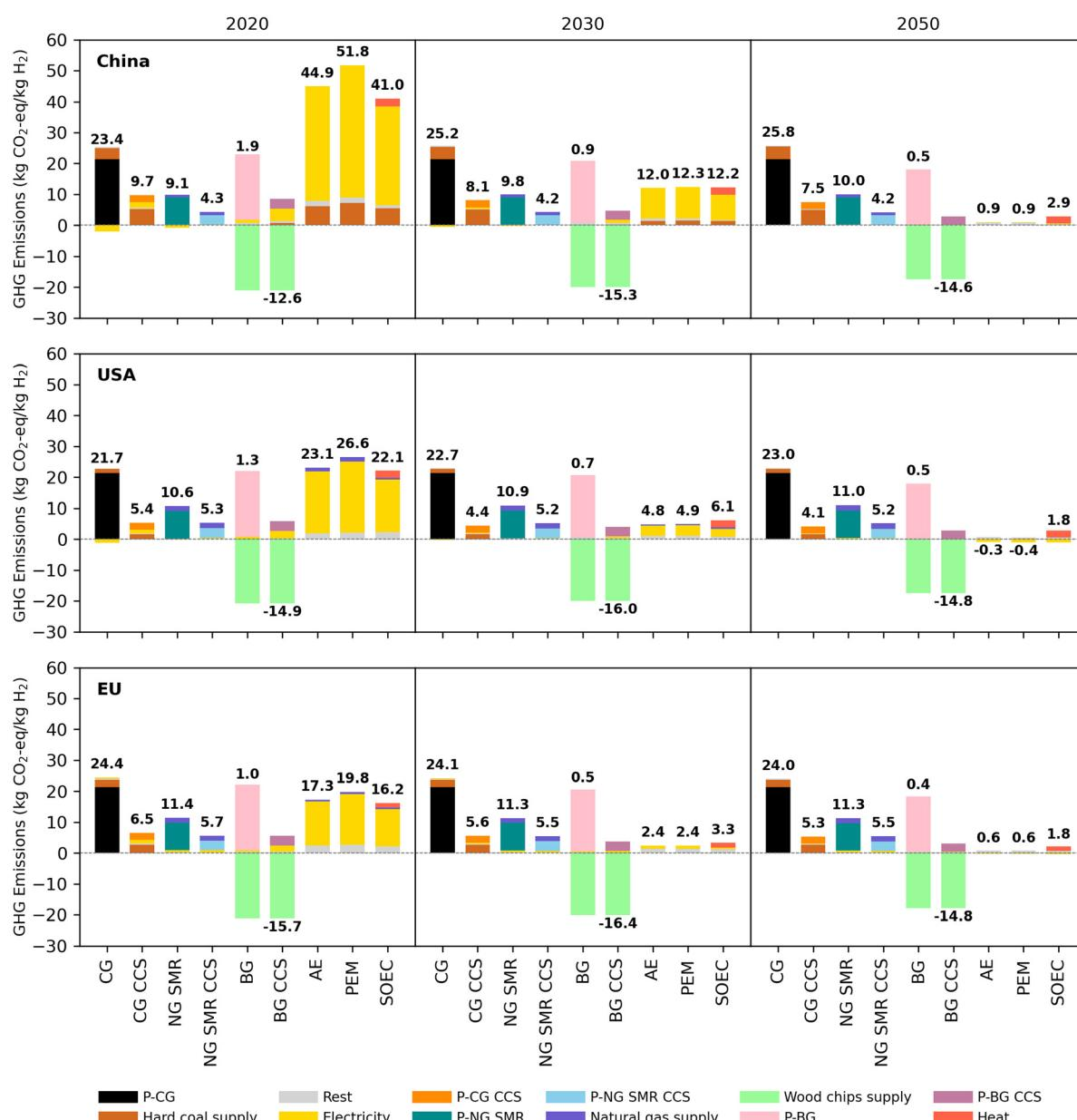


Fig. 2 Contribution analysis of GHG emissions of one kg H<sub>2</sub> production by different technologies in the NZE scenario. In this figure, the prefix P stands for the process itself, CG = coal gasification, NG SMR = steam methane reforming of natural gas, BG = biomass gasification, CCS = carbon capture and storage AE = alkaline electrolyzer, PEM = proton exchange membrane electrolyzer, and SOEC = solid oxide electrolysis cell. In water electrolysis, the coal and natural gas supply are part of the electricity component. For CG and NG SMR, the negative GHG emissions can be generated by electricity co-produced in the H<sub>2</sub> production process when it is assumed to go to the grid. For water electrolysis, the expansion of the bioenergy with CCS in the grid electricity can bring negative emissions.

2030 and 2050. The figure also shows the contributions of different processes to the total global warming potential. The GHG emissions of CG and NG SMR hardly change and increase somewhat over time in China and the USA. One reason for this is that co-produced electricity provides fewer substitution benefits in the future due to a largely decarbonized electricity mix. When CG is coupled with CCS, the overall GHG emissions reduction in 2020 is 59%, 75%, and 73% in China, the USA, and the EU, mainly due to the different regional GHG emissions of coal supply. China has higher GHG emissions per unit of H<sub>2</sub> produced from CG CCS, decreasing from 9.7 kg CO<sub>2</sub>-eq. in 2020 to 7.5 kg CO<sub>2</sub>-eq. in 2050 due to its carbon-intensive coal supply, which is mainly induced by the methane emissions in the mine operation. NG SMR with CCS roughly halves the GHG emissions across all analyzed years. However, it should be noted that GHG emissions of natural gas-based H<sub>2</sub> production are sensitive to upstream fugitive methane leakage rates.<sup>78</sup> For CG and NG SMR, increasing the CO<sub>2</sub> capture rate and reducing the GHG emissions of coal and natural gas supply are likely the most promising routes to further decarbonization.

BG is emphasized among various potential bioenergy-based production routes as it has a high technology readiness level and conversion efficiency.<sup>79</sup> Assuming sustainably managed biomass resources, BG is almost carbon-neutral. A variety of biomass feedstocks could be used, *e.g.*, harvested wood products, agricultural residues, and other biogenic waste fractions.<sup>80</sup> While BG has been modelled from wood chips here, the specific environmental impacts can vary for other production routes. The role of dedicated energy crops should be examined more critically.<sup>81</sup> In the short term, the net GHG emissions reduction of BG CCS is limited partially by electricity use. This reduction grows with electricity decarbonization but eventually declines with efficiency improvements in the BG process (less biomass used to produce one unit of H<sub>2</sub>). While BG with CCS can yield net negative GHG emissions, its role at the global scale is limited by competing biomass uses,<sup>82</sup> land availability, and forest regeneration rates.<sup>83,84</sup> Further, the GHG emissions reduction potential depends on the capture rate and energy consumption of carbon capture.<sup>36</sup> Even under our conservative assumptions, the GHG emissions for transport and storage 1 kg CO<sub>2</sub> are minimal (0.02 CO<sub>2</sub>-eq. currently, and decreasing with electricity decarbonization).

For H<sub>2</sub> production by water electrolysis, the coal- and natural gas-dominated grid electricity currently makes it GHG emissions-intensive. By 2050, significant GHG emissions reduction can be achieved, as high as 98%. This is driven by the decarbonization of the electricity system and efficiency improvements. Due to the dominance of these two factors, the contribution of lifetime extension and material demand decrease of the electrolyzers' stack to the GHG emissions reduction is minimal (less than 1%). The relative contribution of these drivers can be found in the Section 4.1 in ESI.† Compared to the USA and the EU, China experiences the highest GHG emissions reduction for water electrolysis in the future, declining from 45–52 kg CO<sub>2</sub>-eq. per kg H<sub>2</sub> in 2020 to 0.9–2.9 kg CO<sub>2</sub>-eq. per kg H<sub>2</sub> in 2050. This is because China currently has the most carbon-intensive electricity production.

Due to the use of bioenergy with CCS in the power sector, the GHG emissions of water electrolysis in the USA could even become slightly negative in 2050. PEM has the lowest efficiency among the three electrolyzer technologies and has the highest GHG emissions per kg of H<sub>2</sub> produced. However, with the increasing decarbonization of the electricity mix in the future, the differences in GHG emissions between AE, PEM, and SOEC become smaller. As we have assumed the heat for SOEC to originate from a dedicated heat production, the heat used to produce steam causes SOEC to have the highest GHG emissions by 2050. If SOEC was to use waste heat, for example, when integrated with ammonia production,<sup>85</sup> GHG emissions would further decrease.

### 3.2. Prospective environmental impacts of global H<sub>2</sub> production

Decarbonizing global H<sub>2</sub> production can lead to co-benefits and trade-offs with other impact categories. Fig. 3 shows the factor change of environmental impacts per kg H<sub>2</sub> from the global H<sub>2</sub> market in 2030 and 2050 in the three scenarios. In the APS and NZE scenarios, impacts decrease for the following indicators: particulate matter, ozone depletion, and fossil resource depletion. This relates to the energy transition from fossil fuels to renewable electricity, implying a lesser use of fossil fuels and decreased emissions of ozone-depleting gases and fine particles related to their combustion. In the APS, particulate matter emissions increase in the near term due to the slower power transition compared to NZE. In the NZE scenario, ozone depletion slightly increases in the near term due to using a higher share of natural gas-based power and associated emissions of Halons.<sup>86</sup> Near-term eutrophication, photochemical ozone formation, ecotoxicity, and acidification impacts rise due to increased electricity use because of water electrolysis. However, these impacts eventually decline as the power mix shifts predominantly to renewables with minimal nitrogen oxides and sulfur oxides emissions. The increase in human toxicity impacts is tied to the expansion of renewables and the associated release of toxic substances in the environment occurring during the extraction of metals needed to produce photovoltaic panels (*e.g.*, silver, lead, and nickel).<sup>87–89</sup> The increase in impact from ionizing radiation is driven by uranium mining as the nuclear power supply expands.

Across all scenarios, water, land, and resource use (minerals and metals) increase, driven primarily by the water electrolysis scale-up and corresponding infrastructure construction. In addition, the expansion of renewables is responsible for increased land and metals use, such as neodymium and dysprosium for wind turbines or tellurium and indium for photovoltaic panels.<sup>90</sup> Moreover, PEM electrolyzers use platinum and iridium as catalysts to produce H<sub>2</sub>.<sup>91</sup> This technology is regarded as the dominant technology in the future<sup>63</sup> and there may be a considerable demand for water electrolysis in different regions. Today, platinum group metals (*i.e.*, platinum, iridium, palladium, ruthenium) are concentrated in five countries: South Africa, Russia, the USA, Zimbabwe, and Canada. South Africa alone produces around 90% of global platinum and 70% of global iridium



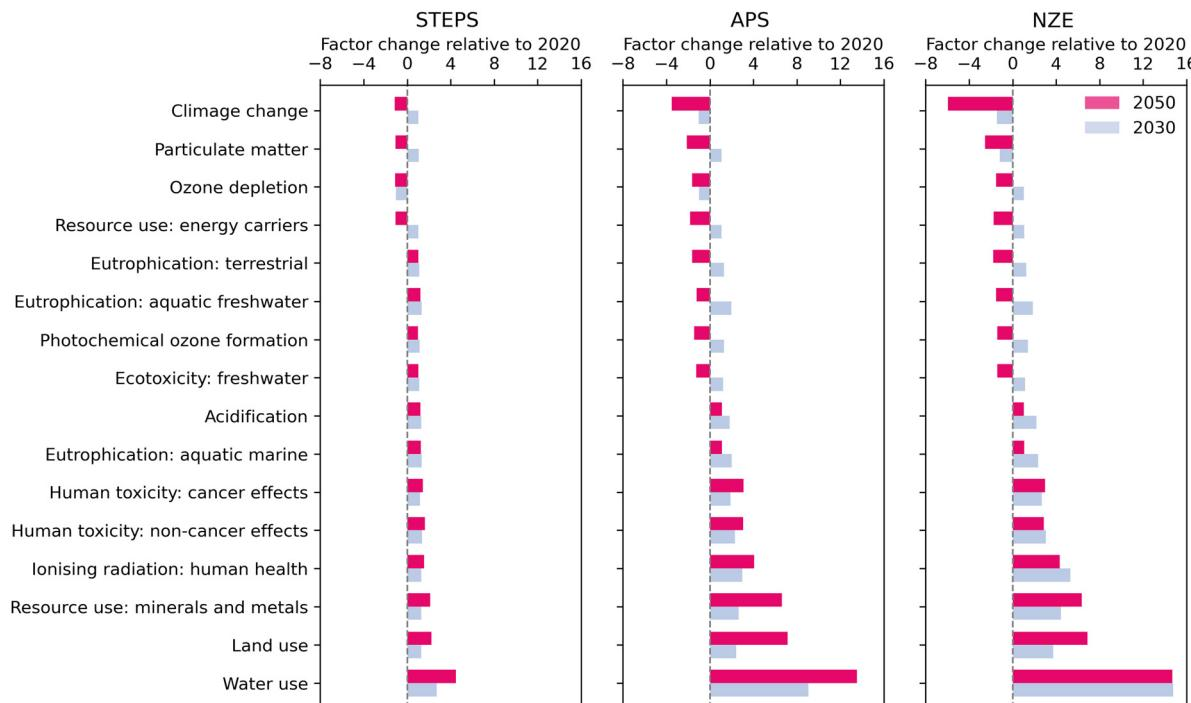


**Fig. 3** The factor change of future environmental impacts of one kg H<sub>2</sub> in the global H<sub>2</sub> market in 2030 and 2050 relative to 2020 in the STEPS, APS, and NZE scenarios. Impact categories excluding climate change are from EF v3.0 method. These values are the weighted average values of different regions. Positive and negative values represent that the environmental impacts will increase and decrease many times in the future compared with 2020. Refer to the Tables S29–S44 in ESI† for global and regional absolute values.

demand.<sup>91,92</sup> An increase in demand for metals may lead to supply risks, especially for rare earth metals.<sup>92–94</sup>

Although water use has the most significant increase among the other indicators per kg of H<sub>2</sub> produced, the overall water use of H<sub>2</sub> production is small relative to other sectors, such as the fossil fuel energy production and the agricultural sector.<sup>95</sup> In the NZE scenario, the total amount of water used as feedstock for the global H<sub>2</sub> production in 2050 is around 4 billion m<sup>3</sup>. This is lower than global water use of fossil fuel energy production in 2021, 19 billion m<sup>3</sup>, and far lower than the global agricultural irrigation water use, 1487 billion m<sup>3</sup>, in 2020.<sup>96,97</sup> The selection of the water cooling technology additionally affects water consumption.<sup>7,98,99</sup> In a wet cooling tower, around 1% of water flow evaporates into the atmosphere. In a once-through cooling system, the withdrawn water is returned, albeit at a higher temperature, potentially affecting aquatic ecosystems.<sup>100</sup> While water use at the global scale should not be a limiting factor for electrolysis, availability could be a limiting factor in specific regions. In locations near the sea, using seawater directly or *via* desalination could be an alternative to using freshwater.<sup>95,101</sup>

It should be pointed out that most of the data used in this study (including the scenario data from REMIND and the IEA) was developed with a perspective on GHG emissions. This means that data for impact categories not directly linked to climate change and the energy transition should not be over-interpreted. For example, technological advancements and environmental improvement measures in metal mining or water management that could reduce impacts in other categories, such as human

toxicity or water use, are not accounted for. Our findings for other impact categories could thus be overestimations and should rather be seen in the light of highlighting areas for potential improvements.

### 3.3. Prospective GHG emissions at regional and global levels

Global annual production volumes of H<sub>2</sub> increase from about 70 Mt per year in 2020 to 121, 263, and 528 Mt in 2050 in the STEPS, APS, and NZE scenarios, respectively (Fig. 4). This corresponds to an increase by a factor 1.7, 3.8, and 7.5. Global GHG emissions of H<sub>2</sub> production are expected to first increase in all scenarios, but then to reduce again in the APS and NZE scenarios, reaching similar emission levels as in 2020, despite much higher H<sub>2</sub> production volumes. In the STEPS scenario there is hardly any change in the technology mix and emissions are dominated by unabated fossil fuel-based H<sub>2</sub> production. In the APS and NZE scenarios CG and NG SMR without CCS decrease and there is a substantial increase of H<sub>2</sub> production *via* water electrolysis (167 Mt and 321 Mt by 2050) and NG SMR CCS (55 Mt and 190 Mt by 2050). While GHG emissions from water electrolysis strongly decrease with the increasing share of renewable power in the electricity mix, the emissions from fossil fuel-based H<sub>2</sub> production are not decarbonized to the same extent. In the NZE scenario, it is expected that after 2040, most H<sub>2</sub> production GHG emissions will come from NG SMR CCS. By 2050, annual GHG emissions from NG SMR CCS are projected to be 0.92 Gt, making up 77% of all H<sub>2</sub> production related GHG emissions. A further reduction of NG SMR CCS



related emissions may be possible if higher CO<sub>2</sub> capture rates and lower energy consumption can be achieved.<sup>102,103</sup>

Across all scenarios, China, the USA, India, the Middle East, and the EU are the key producing regions of H<sub>2</sub>, accounting for

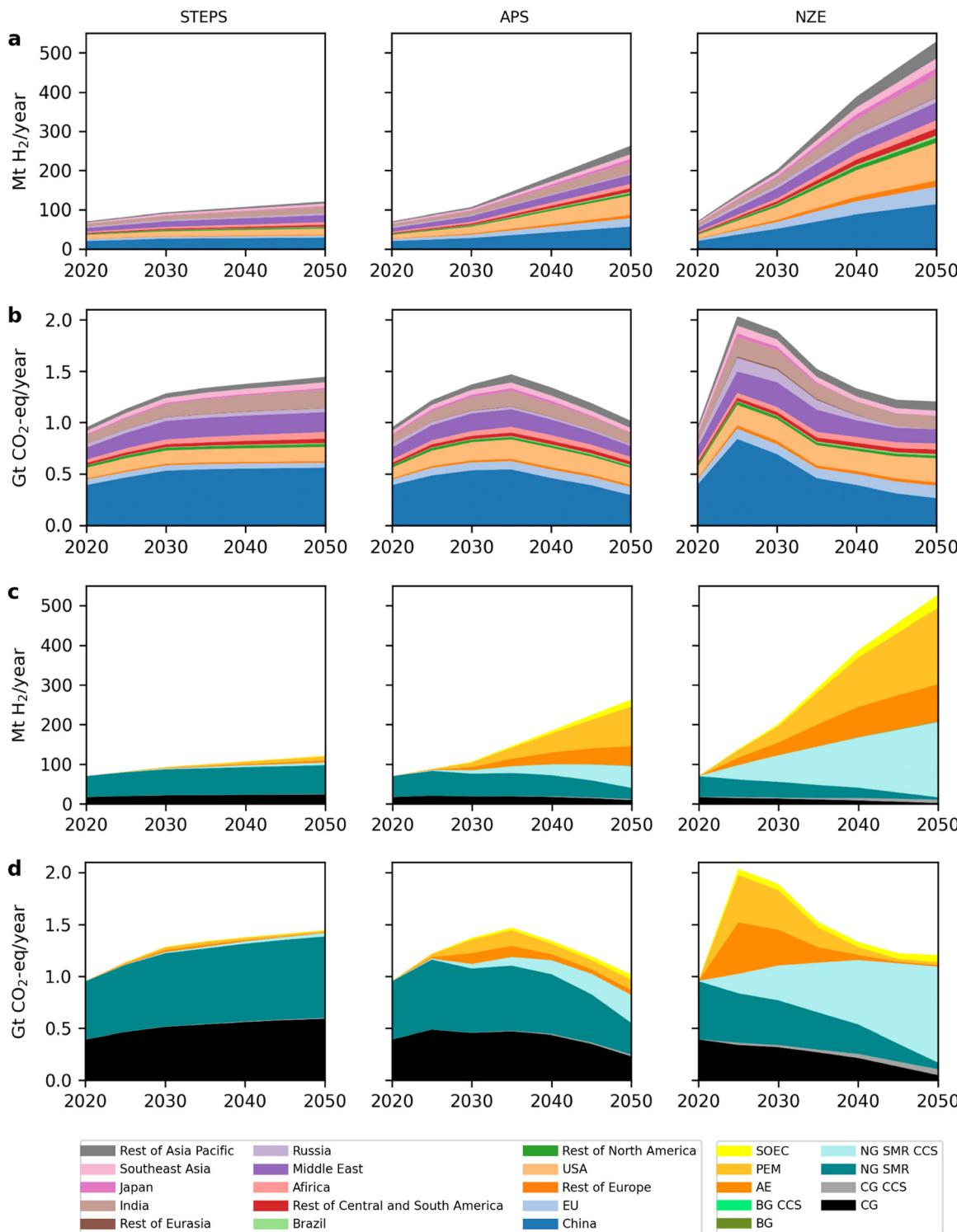


Fig. 4 In three scenarios, the global H<sub>2</sub> production and annual GHG emissions by region and technology from 2020 to 2050. (a) and (b) Show the H<sub>2</sub> production volumes and annual GHG emissions in 15 regions. (c) and (d) Show H<sub>2</sub> production volumes and annual GHG emissions of nine technologies. CG = coal gasification, NG SMR = steam methane reforming of natural gas, BG = biomass gasification, CCS = carbon capture and storage, AE = alkaline electrolyzer, PEM = proton exchange membrane electrolyzer, and SOEC = solid oxide electrolysis cell. The water electrolysis is coupled with grid electricity. Although BG CCS has negative emissions, its final contribution is very small because of its limited adoption.



roughly 70% of the global aggregated H<sub>2</sub> production volume. China will likely remain the largest producer of H<sub>2</sub>, increasing H<sub>2</sub> production from 20 Mt in 2020 to 30–114 Mt in 2050. Currently, most H<sub>2</sub> in China is produced from CG, resulting in a high GHG emissions of 19.1 kg CO<sub>2</sub>-eq. per kg H<sub>2</sub> produced in 2020 (Fig. 5). This is not expected to change substantially in the STEPS scenario. In the APS and NZE scenarios, GHG emissions per kg of H<sub>2</sub> reduce to 5.2 and 2.4 kg CO<sub>2</sub>-eq., respectively, due to a shift towards NG SMR CCS and water electrolysis. This leads to a reduction of China's annual GHG emissions from H<sub>2</sub> production in 2050 in the APS and NZE scenarios of 0.30 Gt and 0.27 Gt, respectively, compared to 0.39 Gt in 2020.

The USA and the EU are expected to increase their H<sub>2</sub> production from 10 Mt and 5 Mt in 2020 to 16–96 Mt and 5–44 Mt in 2050, respectively. Currently, their H<sub>2</sub> production is mostly done *via* NG SMR, resulting in 10.4 and 11.4 kg CO<sub>2</sub>-eq. per kg of H<sub>2</sub>, respectively. These numbers improve to 8.8, 3.4, and 2.4 kg CO<sub>2</sub>-eq. in the USA and 9.9, 3.6, and 2.7 kg CO<sub>2</sub>-eq. in the EU by 2050 for the STEPS, APS and NZE scenarios. The larger improvement in the APS and NZE scenarios is driven by the transition to water electrolysis and NG SMR CCS. Compared to 2020 levels (0.10 Gt for the USA and 0.05 Gt for the EU), annual GHG emissions in 2050 increase to 0.16 Gt and 0.23 Gt in the USA and 0.08 Gt and 0.12 Gt in the EU, in the APS and NZE scenarios, respectively.

### 3.4. Cumulative climate change impacts of H<sub>2</sub> production in the future

To understand the impact of H<sub>2</sub> production at a large scale on the global carbon budget, we quantify the cumulative GHG

emissions of H<sub>2</sub> production from 2020 to 2050.<sup>104</sup> Fig. 6 shows that in 2020, H<sub>2</sub> production emitted 0.95 Gt GHG globally.

Between 2020 and 2050, cumulative GHG emissions from H<sub>2</sub> production are projected at 40 Gt (STEPS), 39 Gt (APS), and 47 Gt (NZE). Despite APS producing four times more H<sub>2</sub> by 2050 than 2020, its emissions are slightly lower than STEPS. The NZE scenario sees a 16% emissions increase compared to the STEPS, but also octuples H<sub>2</sub> production.

Research has shown that the remaining carbon budget for limiting global warming to 1.5 °C with 67% certainty between 2020 and 2050 is about 400 ( $\pm 220$ ) Gt CO<sub>2</sub>-eq.<sup>105</sup> Taking 400 Gt as a basis, the 47 Gt CO<sub>2</sub>-eq. of the NZE scenario amount to 12% of the residual carbon budget (see Section 4.2 in ESI† for regional contributions). This is a very large figure and a faster decarbonization would certainly be desirable.

In the NZE scenario, CG (with and without CCS) contributes 9 Gt (1 Gt and 8 Gt), NG SMR (with and without CCS) contributes 25 Gt (15 Gt and 10 Gt), and water electrolysis contributes to 13 Gt CO<sub>2</sub>-eq. One way to decarbonize faster, would be to power electrolysis to a higher extent by renewables. In our study we have assumed that water electrolysis technologies is powered by average grid electricity. If all electrolysis-based H<sub>2</sub> production was powered entirely by onshore wind energy, global GHG emissions from H<sub>2</sub> production between 2020 and 2050 would be reduced by 2.2%, 9.5%, and 17.9% in the STEPS, APS, and NZE scenarios, respectively (see the ESI† Section 4.3 for more details). This would save about 8 Gt GHG emissions in the NZE scenario. If NG SMR CCS was to be replaced with water electrolysis powered by 100% onshore wind, the overall GHG emissions in the NZE scenario between 2020 and 2050 could be reduced by as much as 12 Gt (26.5%). Together, although somewhat hypothetical, the transition to

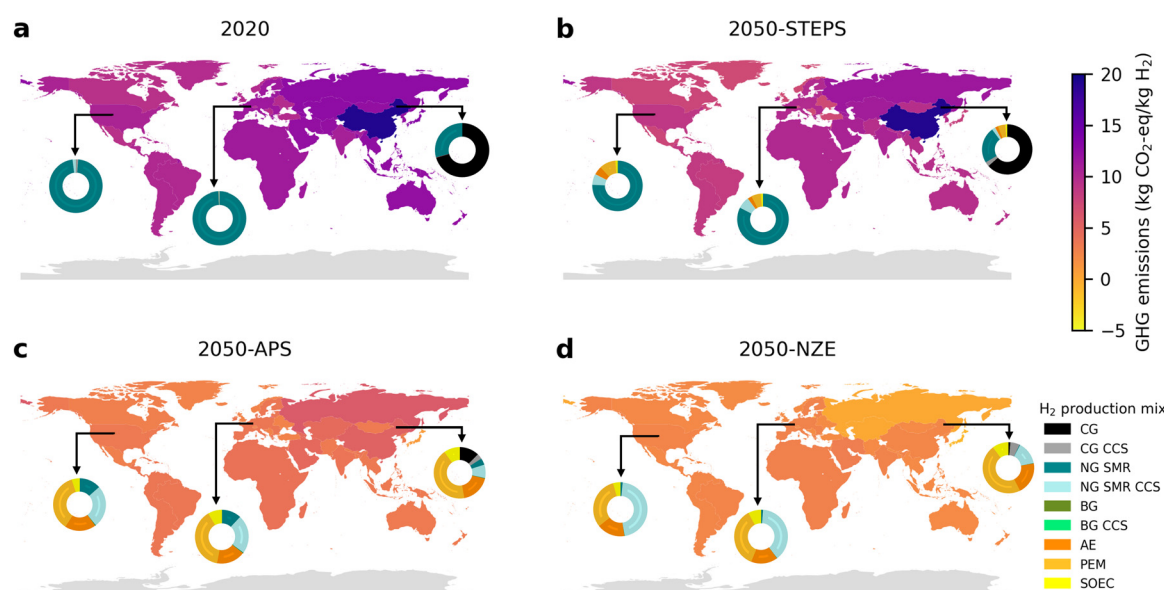


Fig. 5 GHG emissions of one kg H<sub>2</sub> of regional markets in 2020 and 2050. (a) Shows GHG emissions of per kg H<sub>2</sub> from 15 regional H<sub>2</sub> market, as well as market share of different H<sub>2</sub> technologies in China, the USA and the EU in 2020. (b)–(d) show these values in 2050 in three scenarios. In the legend of H<sub>2</sub> production mix, CG = coal gasification, NG SMR = steam methane reforming of natural, BG = biomass gasification, CCS = carbon capture and storage, AE = alkaline electrolyzer, PEM = proton exchange membrane electrolyzer and SOEC = solid oxide electrolysis cell. There is no data for the Antarctic.



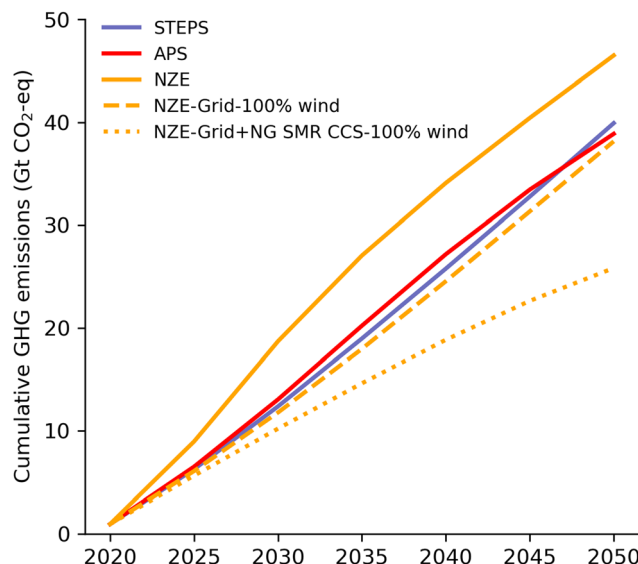


Fig. 6 The cumulative GHG emissions of global H<sub>2</sub> production from 2020 to 2050 in three scenarios.

fully renewable-powered water electrolysis and replacement of NG SMR CCS by the latter could save up to 20 Gt CO<sub>2</sub>-eq. emissions and reduce the cumulative emissions in the NZE scenario by 44.4%.

This analysis shows the tremendous importance of this sector and the need to achieve further GHG emission reductions, if possible beyond that of the NZE scenario. While there is not only one solution, our study shows that an effective way of realizing further reductions would be the further replacement of fossil-based technologies (*e.g.* NG SMR CCS) by water electrolysis with renewable electricity. Our sensitivity analysis does not consider additional infrastructure requirements for storing electricity and H<sub>2</sub> and possible inefficiencies of off-grid insular solutions that might be required to supply H<sub>2</sub> from renewable electricity only. However, the GHG emissions reduction potential from dedicated renewables depends on our ability to develop the additionality, *i.e.* the dedicated renewable power generation capacity for H<sub>2</sub> production,<sup>106,107</sup> faster than projected. It is worth noting that increasing H<sub>2</sub> production from electrolysis and renewable electricity implies significant investment. For example, to produce more than 3 Mt of clean H<sub>2</sub> per year by 2030, the U.S. Department of Energy has announced 7 billion to support seven regional clean H<sub>2</sub> hubs, which is to be met by private sector investments of 40 billion.<sup>108</sup> Thus, without significant investments by public and private stakeholders, H<sub>2</sub> production may not develop as fast as desired.

## 4. Conclusions

In this work, we systematically assess the environmental impacts of future H<sub>2</sub> production technologies until 2050 at the regional and global levels. The assessment includes important drivers of impacts, such as electricity decarbonization, efficiency improvements, advancements in electrolyzer technology, the use of CCS,

and changes in the H<sub>2</sub> production mix. The IEA scenarios reflect possible consequences of current policy settings (STEPS), realizing all climate commitments in addition to already implemented policy (APS) and achieving net zero CO<sub>2</sub> emissions by 2050 (NZE). Our results can inform policy makers on the potential magnitude of future environmental impacts related to an increasing H<sub>2</sub> production and options to reduce them further. Our study also provides GHG emission intensities (and the underlying LCI data) of current and future H<sub>2</sub> production technologies that can be used to assess the GHG emissions mitigation potential of H<sub>2</sub> in different sectors. Our main conclusions are the following:

### H<sub>2</sub> production needs to shift away from fossil fuels

Water electrolysis will have the steepest decrease in GHG emissions per kg H<sub>2</sub> output between 2020 and 2050, mainly driven by electricity decarbonization and efficiency improvements. Despite variations across regions (*i.e.*, China, the USA, and the EU) due to different renewables deployment strategies, emissions reduce to almost zero in 2050 in the NZE scenario, regardless of the electrolyzer type. In contrast, traditional H<sub>2</sub> pathways (*i.e.*, CG and NG SMR) have much higher GHG emissions per kg H<sub>2</sub> produced. Even with CCS GHG emissions are considerably higher. In fact, in all analyzed scenarios fossil fuel technologies still dominate climate change impacts by 2050. The investment into additional NG SMR CCS capacities seem questionable from a GHG perspective, as shown in the NZE scenario, and could create a risky fossil fuel lock-in.<sup>109</sup> This conclusion is unlikely to change, unless very high capture rates in CCS can be achieved. Given that there is also uncertainty about whether CCS can be deployed at the required scale and locations,<sup>110</sup> a shift towards more electrolysis and renewable electricity seems to be a safer, more climate friendly and future-proof option.

### H<sub>2</sub> production related GHG emissions need to be further minimized and avoid the carbon lock-in risk from CCS

Although the development of a H<sub>2</sub> economy is being promoted with the aim to reduce GHG emissions in different sectors,<sup>111</sup> our analysis shows that in the NZE scenario the production of H<sub>2</sub> alone could consume up to 2050 as much as 12% (47 Gt CO<sub>2</sub>-eq.) of the remaining carbon budget to meet the 1.5 °C target. This is a staggering quantity of GHG emissions and calls for a faster decarbonization than projected in the analyzed scenarios. This is largely due to NG SMR CCS. CCS only can be expected to have an overall capturing efficiency of 64% for NG SMR. Therefore, NG SMR CCS is almost fully responsible for the 1 Gt CO<sub>2</sub>-eq. per year emitted by 2050 for H<sub>2</sub> production. Since the CCS infrastructure is being build up from 2020 and likely will have a significant remaining technical life time, this will lock in additional carbon emissions at this level for years if not decades after 2050. As discussed, the most promising route seems a more rapid transition to electrolysis based H<sub>2</sub> production from renewable electricity, which could reduce cumulative GHG emissions by 2050 to 27 Gt (6.8% of the remaining carbon budget). This would, however, require a faster expansion of



renewable electricity generation capacities as assumed in our scenarios.

### Environmental trade-offs should be further examined and minimized

As CCS and water electrolysis rely increasingly on low-carbon electricity, there are likely co-benefits with other indicators such as particulate matter formation, ozone depletion, and fossil resource depletion. Concomitantly, other indicators could worsen, such as water use, land use, resource extraction and human toxicity. This is mainly due to the scale-up of water electrolysis and the use of renewable electricity. While electrolysis will require considerable amounts of water at the global scale, these amounts are small compared to the global use of water for agriculture. However, for certain regions with high water stress, its feasibility should be critically examined.<sup>112</sup> Electrolyzers and renewables will require substantial quantities of metals, however, it has also been shown that the energy transition may substantially reduce the overall mining activity.<sup>89</sup> As rare earth metals required by PEM are concentrated in specific countries, the supply risk of these metals in some regions should be carefully assessed before promoting this technology. Toxicity and other environmental impacts related to mining and metal production can also be reduced through improved technologies and better management,<sup>113,114</sup> which has not been considered here. Further assessments of specific H<sub>2</sub> production technologies and related environmental impacts should be conducted to anticipate and minimize undesired trade-offs locally and at the global scale.

### Further research needs

The leading H<sub>2</sub> technologies considered by the IEA are assessed in this paper. In addition, the environmental impacts of other promising technologies, such as photocatalytic water splitting,<sup>115,116</sup> should be further assessed. Further research should be done to assess the potential GHG mitigation effects of using H<sub>2</sub> in hard-to-abate sectors (like cement, iron and steel and heavy transport, *etc.*) and related environmental benefits or trade-offs at the global scale.<sup>111</sup> The future scenarios for the H<sub>2</sub> production and unit process data presented here may serve as a basis for such analyses.

## Abbreviations

AE	Alkaline electrolyzers
APS	Announced pledges scenario
BG	Biomass gasification
BG CCS	Biomass gasification with carbon capture and storage
BoP	Balance of plant
CCS	Carbon capture and storage
CG	Coal gasification
CG CCS	Coal gasification with carbon capture and storage
CO	Carbon monoxide
CO <sub>2</sub>	Carbon dioxide
GHG	Greenhouse gas
H <sub>2</sub>	Hydrogen

H2A	Hydrogen analysis production models
IAM	Integrated assessment model
IEA	International energy agency
IPCC	Intergovernmental panel on climate change
LCA	Life-cycle assessment
LCI	Life cycle inventory
MDEA	Methyl diethanolamine
NG SMR	Steam reforming of natural gas
NG SMR CCS	Steam reforming of natural gas with carbon capture and storage
NZE	Net zero emissions by 2050 scenario
PEM	Proton exchange membrane electrolyzers
PSA	Pressure swing adsorption
REMIND	Regional model of investments and development
SOEC	Solid oxide electrolysis cell
SSP	Shared socioeconomic pathway
STEPS	Stated policies scenario
WGSR	Water-gas shift reaction

## Conflicts of interest

There are no conflicts to declare.

## Acknowledgements

The authors thank Dr Simon Bennett (IEA) for sharing data about H<sub>2</sub> production amounts in the future. The authors further thank Dr Vassilis Daioglou (PBL) for the insight of H<sub>2</sub> in the IAM model. The authors also thank Maarten van 't Zelfde (CML) for his help with GIS. The authors also thank the anonymous reviewers for their constructive feedback. This work is supported by the China Scholarship Council (Grant No. 202006430008). Dr Romain Sacchi has received financial support *via* the research project SHELTERED, funded by the Swiss Federal Office of Energy (SFOE).

## References

- IPCC, Global Warming of 1.5 °C: IPCC Special Report on Impacts of Global Warming of 1.5 °C above Pre-industrial Levels in Context of Strengthening Response to Climate Change, Sustainable Development, and Efforts to Eradicate Poverty, Report 9781009157957, Intergovernmental Panel on Climate Change, Cambridge, 2018.
- IEA, Net Zero by 2050, *International Energy Agency*, 2021.
- I. Staffell, D. Scamman, A. Velazquez Abad, P. Balcombe, P. E. Dodds, P. Ekins, N. Shah and K. R. Ward, *Energy Environ. Sci.*, 2019, **12**, 463–491.
- IEA, Global Hydrogen Review 2021, International Energy Agency, Paris, 2021.
- A. Odenweller, F. Ueckerdt, G. F. Nemet, M. Jensterle and G. Luderer, *Nat. Energy*, 2022, **7**, 854–865.



6 C. F. Blanco, S. Cucurachi, J. B. Guinée, M. G. Vijver, W. J. G. M. Peijnenburg, R. Trattnig and R. Heijungs, *J. Cleaner Prod.*, 2020, **259**, 120968.

7 T. Weidner, V. Tulus and G. Guillén-Gosálbez, *Int. J. Hydrogen Energy*, 2023, **48**, 8310–8327.

8 J. B. Guinée, R. Heijungs, G. Huppes, A. Zamagni, P. Masoni, R. Buonamici, T. Ekwall and T. Rydberg, *Environ. Sci. Technol.*, 2011, **45**, 90–96.

9 R. Bhandari, C. A. Trudewind and P. Zapp, *J. Cleaner Prod.*, 2014, **85**, 151–163.

10 O. Siddiqui and I. Dincer, *Int. J. Hydrogen Energy*, 2019, **44**, 5773–5786.

11 G. Palmer, A. Roberts, A. Hoadley, R. Dargaville and D. Honnery, *Energy Environ. Sci.*, 2021, **14**, 5113–5131.

12 C. Bauer, K. Treyer, C. Antonini, J. Bergerson, M. Gazzani, E. Gencer, J. Gibbins, M. Mazzotti, S. T. McCoy, R. McKenna, R. Pietzcker, A. P. Ravikumar, M. C. Romano, F. Ueckerdt, J. Vente and M. van der Spek, *Sustainable Energy Fuels*, 2022, **6**, 66–75.

13 A. Valente, D. Iribarren and J. Dufour, *Int. J. Life Cycle Assess.*, 2017, **22**, 346–363.

14 M. Delpierre, J. Quist, J. Mertens, A. Prieur-Vernat and S. Cucurachi, *J. Cleaner Prod.*, 2021, **299**, 126866.

15 P. Lamers, T. Ghosh, S. Upasani, R. Sacchi and V. Daioglou, *Environ. Sci. Technol.*, 2023, **57**, 2464–2473.

16 R. Sacchi, T. Terlouw, K. Siala, A. Dirnaichner, C. Bauer, B. Cox, C. Mutel, V. Daioglou and G. Luderer, *Renewable Sustainable Energy Rev.*, 2022, **160**, 112311.

17 L. Baumstark, N. Bauer, F. Benke, C. Bertram, S. Bi, C. C. Gong, J. P. Dietrich, A. Dirnaichner, A. Giannousakis, J. Hilaire, D. Klein, J. Koch, M. Leimbach, A. Levesque, S. Madeddu, A. Malik, A. Merfort, L. Merfort, A. Odenweller, M. Pehl, R. C. Pietzcker, F. Piontek, S. Rauner, R. Rodrigues, M. Rottoli, F. Schreyer, A. Schultes, B. Soergel, D. Soergel, J. Strefler, F. Ueckerdt, E. Kriegler and G. Luderer, *Geosci. Model Dev.*, 2021, **14**, 6571–6603.

18 IEA, World Energy Outlook 2022, International Energy Agency, Paris, 2022.

19 IEA, Hydrogen in Latin America: From near-term opportunities to large-scale deployment, International Energy Agency, Paris, 2021.

20 IEA, Hydrogen Production Projects Database, International Energy Agency, Paris, 2022.

21 NREL, Current Hydrogen from Coal without CO<sub>2</sub> Capture and Sequestration, <https://www.nrel.gov/hydrogen/assets/docs/current-central-coal-without-co2-sequestration-v2-1-1.xls>, (accessed 4th May, 2022).

22 A. Wokaun and E. Wilhelm, *Transition to Hydrogen: Pathways toward Clean Transportation*, Cambridge University Press, Cambridge, 2011.

23 IEA, The Future of Hydrogen, International Energy Agency, Paris, 2019.

24 NREL, Current Central Hydrogen from Coal with CO<sub>2</sub> Capture and Sequestration, <https://www.nrel.gov/hydrogen/h2a-production-models.html>, (accessed 4th May, 2022).

25 K. Volkart, C. Bauer and C. Boulet, *Int. J. Greenhouse Gas Control*, 2013, **16**, 91–106.

26 C. Antonini, K. Treyer, A. Streb, M. van der Spek, C. Bauer and M. Mazzotti, *Sustainable Energy Fuels*, 2020, **4**, 2967–2986.

27 C. Antonini, K. Treyer, E. Moioli, C. Bauer, T. J. Schildhauer and M. Mazzotti, *Sustainable Energy Fuels*, 2021, **5**, 2602–2621.

28 DEA, Technology Data for Renewable Fuels, Danish Energy Agency, 2022.

29 N. Gerloff, *J. Energy Storage*, 2021, **43**, 102759.

30 R. Kothari, D. Buddhi and R. L. Sawhney, *Renewable Sustainable Energy Rev.*, 2008, **12**, 553–563.

31 F. Mueller-Langer, E. Tzimas, M. Kaltschmitt and S. Petev, *Int. J. Hydrogen Energy*, 2007, **32**, 3797–3810.

32 IPCC, Carbon Dioxide Capture and Storage, Intergovernmental Panel on Climate Change, New York, 2005.

33 J. Alcalde, S. Flude, M. Wilkinson, G. Johnson, K. Edlmann, C. E. Bond, V. Scott, S. M. V. Gilfillan, X. Ogaya and R. S. Haszeldine, *Nat. Commun.*, 2018, **9**, 2201.

34 R. Heijungs, K. Allacker, E. Benetto, M. Brandão, J. Guinée, S. Schaubroeck, T. Schaubroeck and A. Zamagni, *Front. Sustainability*, 2021, **2**.

35 Á. Galán-Martín, V. Tulus, I. Díaz, C. Pozo, J. Pérez-Ramírez and G. Guillén-Gosálbez, *One Earth*, 2021, **4**, 565–583.

36 B. Singh, A. H. Strømman and E. G. Hertwich, *Int. J. Greenhouse Gas Control*, 2011, **5**, 911–921.

37 DEA, Technology Data for Carbon Capture, Transport and Storage Danish Energy Agency, Copenhagen, 2021.

38 A. Aspelund and K. Jordal, *Int. J. Greenhouse Gas Control*, 2007, **1**, 343–354.

39 F. Donda, V. Volpi, S. Persoglia and D. Parushev, *Int. J. Greenhouse Gas Control*, 2011, **5**, 327–335.

40 IEAGHG, The Costs of CO<sub>2</sub> Storage – Post-demonstration CCS in the EU, Brussels, 2019.

41 V. Vishal, *Fuel*, 2017, **192**, 201–207.

42 B. Parkinson, M. Tabatabaei, D. C. Upham, B. Ballinger, C. Greig, S. Smart and E. McFarland, *Int. J. Hydrogen Energy*, 2018, **43**, 2540–2555.

43 IEAGHG, Techno-Economic Evaluation of SMR Based Standalone (Merchant) Hydrogen Plant with CCS, The IEA Greenhouse Gas R&D Programme, 2017.

44 P. Nikolaidis and A. Poullikkas, *Renewable Sustainable Energy Rev.*, 2017, **67**, 597–611.

45 D. Hospital-Benito, I. Díaz and J. Palomar, *Sustain. Prod. Consum.*, 2023, **38**, 283–294.

46 S. Fuss, J. G. Canadell, G. P. Peters, M. Tavoni, R. M. Andrew, P. Ciais, R. B. Jackson, C. D. Jones, F. Kraxner, N. Nakicenovic, C. Le Quéré, M. R. Raupach, A. Sharifi, P. Smith and Y. Yamagata, *Nat. Clim. Change*, 2014, **4**, 850–853.

47 Y. X. Chen, A. Lavacchi, H. A. Miller, M. Bevilacqua, J. Filippi, M. Innocenti, A. Marchionni, W. Oberhauser, L. Wang and F. Vizza, *Nat. Commun.*, 2014, **5**, 4036.

48 G. Zhao, M. R. Kraglund, H. L. Frandsen, A. C. Wulff, S. H. Jensen, M. Chen and C. R. Graves, *Int. J. Hydrogen Energy*, 2020, **45**, 23765–23781.

49 K. E. Ayers, C. Capuano and E. B. Anderson, *ECS Trans.*, 2012, **41**, 15.



50 A. H. Reksten, M. S. Thomassen, S. Møller-Holst and K. Sundseth, *Int. J. Hydrogen Energy*, 2022, **47**, 38106–38113.

51 R. J. Ouimet, J. R. Glenn, D. De Porcellinis, A. R. Motz, M. Carmo and K. E. Ayers, *ACS Catal.*, 2022, **12**, 6159–6171.

52 M. A. Laguna-Bercero, *J. Power Sources*, 2012, **203**, 4–16.

53 G. Lo Basso, A. Mojtahehd, L. M. Pastore and L. De Santoli, *Int. J. Hydrogen Energy*, 2024, **52**, 978–993.

54 E. R. Morgan, J. F. Manwell and J. G. McGowan, *Int. J. Hydrogen Energy*, 2013, **38**, 15903–15909.

55 M. H. Ali Khan, R. Daiyan, Z. Han, M. Hablitzel, N. Haque, R. Amal and I. MacGill, *iScience*, 2021, **24**, 102539.

56 K. Bareiß, C. de la Rua, M. Möckl and T. Hamacher, *Appl. Energy*, 2019, **237**, 862–872.

57 A. Simons and C. Bauer, *Appl. Energy*, 2015, **157**, 884–896.

58 IRENA, Green Hydrogen Cost Reduction: Scaling up Electrolysers to Meet the 1.5 °C Climate Goal, International Renewable Energy Agency, Abu Dhabi, 2020.

59 FCE, FuelCell Energy Announces Solid Oxide Electrolysis and Fuel Cell Platform to Improve Control and Flexibility of Energy Investments, FuelCell Energy, Inc., 2022.

60 R. E. Lester, D. Gunasekera, W. Timms and D. Downie, Water requirements for use in hydrogen production in Australia: Potential public policy and industry-related issues, Deakin University, 2022.

61 GCCSI, Replacing 10% of NSW Natural Gas Supply with Clean Hydrogen: Comparison of Hydrogen Production Options, Global CCS Institute, Melbourne, 2020.

62 IEA, The Future of Hydrogen - Seizing today's opportunities, International Energy Agency, 2019.

63 O. Schmidt, A. Gambhir, I. Staffell, A. Hawkes, J. Nelson and S. Few, *Int. J. Hydrogen Energy*, 2017, **42**, 30470–30492.

64 NREL, H2A: Hydrogen Analysis Production Models, <https://www.nrel.gov/hydrogen/h2a-production-models.html>, (accessed 10th, December, 2023).

65 IEA, Global Energy and Climate Model International Energy Agency, 2022.

66 IEA, Global Hydrogen Review 2022, International Energy Agency, Paris, 2022.

67 R. Arvidsson, A.-M. Tillman, B. A. Sandén, M. Janssen, A. Nordelöf, D. Kushnir and S. Molander, *J. Ind. Ecol.*, 2018, **22**, 1286–1294.

68 A. Mendoza Beltran, B. Cox, C. Mutel, D. P. van Vuuren, D. Font Vivanco, S. Deetman, O. Y. Edelenbosch, J. Guinée and A. Tukker, *J. Ind. Ecol.*, 2020, **24**, 64–79.

69 K. Riahi, D. P. van Vuuren, E. Kriegler, J. Edmonds, B. C. O'Neill, S. Fujimori, N. Bauer, K. Calvin, R. Dellink, O. Frick, W. Lutz, A. Popp, J. C. Cuaresma, S. Kc, M. Leimbach, L. Jiang, T. Kram, S. Rao, J. Emmerling, K. Ebi, T. Hasegawa, P. Havlik, F. Humpenöder, L. A. Da Silva, S. Smith, E. Stehfest, V. Bosetti, J. Eom, D. Gernaat, T. Masui, J. Rogelj, J. Strefler, L. Drouet, V. Krey, G. Luderer, M. Harmsen, K. Takahashi, L. Baumstark, J. C. Doelman, M. Kainuma, Z. Klimont, G. Marangoni, H. Lotze-Campen, M. Obersteiner, A. Tabeau and M. Tavoni, *Global Environ. Change*, 2017, **42**, 153–168.

70 O. Frick, P. Havlik, J. Rogelj, Z. Klimont, M. Gusti, N. Johnson, P. Kolp, M. Strubegger, H. Valin, M. Amann, T. Ermolieva, N. Forsell, M. Herrero, C. Heyes, G. Kindermann, V. Krey, D. L. McCollum, M. Obersteiner, S. Pachauri, S. Rao, E. Schmid, W. Schoepp and K. Riahi, *Global Environ. Change*, 2017, **42**, 251–267.

71 J. Rogelj, A. Popp, K. V. Calvin, G. Luderer, J. Emmerling, D. Gernaat, S. Fujimori, J. Strefler, T. Hasegawa, G. Marangoni, V. Krey, E. Kriegler, K. Riahi, D. P. van Vuuren, J. Doelman, L. Drouet, J. Edmonds, O. Frick, M. Harmsen, P. Havlik, F. Humpenöder, E. Stehfest and M. Tavoni, *Nat. Clim. Change*, 2018, **8**, 325–332.

72 G. Wernet, C. Bauer, B. Steubing, J. Reinhard, E. Moreno-Ruiz and B. Weidema, *Int. J. Life Cycle Assess.*, 2016, **21**, 1218–1230.

73 IPCC, Climate Change 2013 – The Physical Science Basis: Working Group I Contribution to the Fifth Assessment Report of the Intergovernmental Panel on Climate Change, Report 9781107057999, Intergovernmental Panel on Climate Change, Cambridge, 2013.

74 N. Warwick, P. Griffiths, J. Keeble, A. Archibald, J. Pyle and K. Shine, Atmospheric implications of increased Hydrogen use, Department for Business, Energy and Industrial Strategy, 2022.

75 S. Fazio, F. Biganzoli, V. De Laurentiis, L. Zampori and S. D. Sala, *E*, Supporting information to the characterisation factors of recommended EF Life Cycle Impact Assessment methods, Version 2, from ILCD to EF 3.0, European Commission, Ispra, 2018.

76 B. Steubing, D. de Koning, A. Haas and C. L. Mutel, *Softw. Impacts*, 2020, **3**, 100012.

77 B. Steubing and D. de Koning, *Int. J. Life Cycle Assess.*, 2021, **26**, 2248–2262.

78 R. W. Howarth and M. Z. Jacobson, *Energy Sci. Eng.*, 2021, **9**, 1676–1687.

79 T. Lepage, M. Kammoun, Q. Schmetz and A. Richel, *Biomass Bioenergy*, 2021, **144**, 105920.

80 EBA, Decarbonising Europe's hydrogen production with biohydrogen, European Biogas Association, Brussels, 2023.

81 J. P. W. Scharlemann and W. F. Laurance, *Science*, 2008, **319**, 43–44.

82 R. Birdsey, P. Duffy, C. Smyth, W. A. Kurz, A. J. Dugan and R. Houghton, *Environ. Res. Lett.*, 2018, **13**, 050201.

83 K. Navare, W. Arts, G. Faraca, G. V. D. Bossche, B. Sels and K. V. Acker, *Resour., Conserv. Recycl.*, 2022, **186**, 106588.

84 M. van der Spek, C. Banet, C. Bauer, P. Gabrielli, W. Goldthorpe, M. Mazzotti, S. T. Munkejord, N. A. Røkke, N. Shah, N. Sunny, D. Sutter, J. M. Trusler and M. Gazzani, *Energy Environ. Sci.*, 2022, **15**, 1034–1077.

85 J. B. Hansen, Topsoe's Road Map to All Electric Ammonia Plants, Pittsburgh, 2018.

86 B. Atilgan and A. Azapagic, *J. Cleaner Prod.*, 2015, **106**, 555–564.

87 M. Tammaro, A. Salluzzo, J. Rimauro, S. Schiavo and S. Manzo, *J. Hazard. Mater.*, 2016, **306**, 395–405.

88 K. Treyer, C. Bauer and A. Simons, *Energy Policy*, 2014, **74**, S31–S44.

89 J. Nijnens, P. Behrens, O. Kraan, B. Sprecher and R. Kleijn, *Joule*, 2023, **7**, 2408–2413.



90 G. Luderer, M. Pehl, A. Arvesen, T. Gibon, B. L. Bodirsky, H. S. de Boer, O. Fricko, M. Hejazi, F. Humpenöder, G. Iyer, S. Mima, I. Mouratiadou, R. C. Pietzcker, A. Popp, M. van den Berg, D. van Vuuren and E. G. Hertwich, *Nat. Commun.*, 2019, **10**, 5229.

91 C. Minke, M. Suermann, B. Bensmann and R. Hanke-Rauschenbach, *Int. J. Hydrogen Energy*, 2021, **46**, 23581–23590.

92 K. D. Rasmussen, H. Wenzel, C. Bangs, E. Petavratzi and G. Liu, *Environ. Sci. Technol.*, 2019, **53**, 11541–11551.

93 A. Månberger and B. Johansson, *Energy Strategy Rev.*, 2019, **26**, 100394.

94 R. Fu, K. Peng, P. Wang, H. Zhong, B. Chen, P. Zhang, Y. Zhang, D. Chen, X. Liu, K. Feng and J. Li, *Nat. Commun.*, 2023, **14**, 3703.

95 R. R. Beswick, A. M. Oliveira and Y. Yan, *ACS Energy Lett.*, 2021, **6**, 3167–3169.

96 FAO, AQUASTAT, United Nations Food and Agriculture Organization, 2024.

97 IEA, Clean energy can help to ease the water crisis, International Energy Agency, Paris, 2023.

98 WaterSMART, Water for the Hydrogen Economy, Calgary, 2020.

99 K. T. Solutions, Hydrogen Production & Distribution, (accessed 16th December, 2023).

100 C. E. Raptis, J. M. Boucher and S. Pfister, *Sci. Total Environ.*, 2017, **580**, 1014–1026.

101 H. Xie, Z. Zhao, T. Liu, Y. Wu, C. Lan, W. Jiang, L. Zhu, Y. Wang, D. Yang and Z. Shao, *Nature*, 2022, **612**, 673–678.

102 M. N. Dods, E. J. Kim, J. R. Long and S. C. Weston, *Environ. Sci. Technol.*, 2021, **55**, 8524–8534.

103 P. Brandl, M. Bui, J. P. Hallett and N. Mac Dowell, *Int. J. Greenhouse Gas Control*, 2021, **105**, 103239.

104 H. D. Matthews, K. Zickfeld, R. Knutti and M. R. Allen, *Environ. Res. Lett.*, 2018, **13**, 010201.

105 IPCC, Climate Change 2022: Mitigation of Climate Change, Intergovernmental Panel on Climate Change, 2022.

106 C. Delft, Additionality of renewable electricity for green hydrogen production in the EU, CE Delft, Delft, 2022.

107 M. A. Giovanniello, A. N. Cybulsky, T. Schittekatte and D. S. Mallapragada, *Nat. Energy*, 2024, DOI: [10.1038/s41560-023-01435-0](https://doi.org/10.1038/s41560-023-01435-0).

108 US-DOE, Biden-Harris Administration Announces 7 Billion For America's First Clean Hydrogen Hubs, Driving Clean Manufacturing and Delivering New Economic Opportunities Nationwide, <https://www.energy.gov/articles/biden-harris-administration-announces-7-billion-americas-first-clean-hydrogen-hubs-driving>, (accessed 11th December, 2023).

109 P. J. Vergragt, N. Markussen and H. Karlsson, *Global Environ. Change*, 2011, **21**, 282–292.

110 E. Martin-Roberts, V. Scott, S. Flude, G. Johnson, R. S. Haszeldine and S. Gilfillan, *One Earth*, 2021, **4**, 1569–1584.

111 X. Yang, C. P. Nielsen, S. Song and M. B. McElroy, *Nat. Energy*, 2022, **7**, 955–965.

112 D. Tonelli, L. Rosa, P. Gabrielli, K. Caldeira, A. Parente and F. Contino, *Nat. Commun.*, 2023, **14**, 5532.

113 G. Wang, J. Xu, L. Ran, R. Zhu, B. Ling, X. Liang, S. Kang, Y. Wang, J. Wei, L. Ma, Y. Zhuang, J. Zhu and H. He, *Nat. Sustainability*, 2023, **6**, 81–92.

114 S. H. Farjana, N. Huda, M. A. Parvez Mahmud and R. Saidur, *J. Cleaner Prod.*, 2019, **231**, 1200–1217.

115 S. Guo, X. Li, J. Li and B. Wei, *Nat. Commun.*, 2021, **12**, 1343.

116 M. Z. Rahman and J. Gascon, *Chem. Catal.*, 2023, **3**, 100536.

